View metadata, citation and similar papers at core.ac.uk

brought to you by CORE

provided by Repository of the Academy's Library

This document is the Accepted Manuscript version of a Published Work that appeared in final form in *J. Chem. Phys.* **125**, 064501 (2006)**, copyright © American Institute of Physics after peer review and technical editing by the publisher. To access the final edited and published work see**

jcp.aip.org

Quantized time correlation function approach to non-adiabatic decay rates in condensed phase: Application to solvated electrons in water and methanol

Daniel Borgis[a,d] , Peter J. Rossky[b,d] and László Turi[c,d]

[a]*Département Physique et Modélisation, Université d'Evry-Val-d'Essone, Bd. François Mitterand, 91025 Evry, France*

[b]*Department of Chemistry and Biochemistry, Institute for Theoretical Chemistry, University of Texas at Austin, Austin, TX 78712-1167*

[c]*Department of Physical Chemistry, Eötvös Loránd University, Budapest 112, P.O.Box 32, Hungary, H-1518*

Abstract: A new, alternative form of the golden rule formula defining the non-adiabatic transition rate between two quantum states in condensed phase is presented. The formula involves the quantum time correlation function of the energy gap, of the non-adiabatic coupling, and their cross terms. Those quantities can be inferred from their classical counterparts, determined via MD simulations. The formalism is applied to the problem of the non-adiabatic $p \rightarrow s$ relaxation of an equilibrated p-electron in water and methanol. We find that, in both solvent, the relaxation is induced by the coupling to the vibrational modes and the quantum effects modify the rate by a factor of 2-10 depending on the quantization procedure applied. The resulting p-state lifetime for a hypothetical equilibrium excited state appears extremely short, in the sub-100 fs regime. Although this result is in contrast with all previous theoretical predictions, we also illustrate that the lifetimes computed here are very sensitive to the simulated electronic quantum gap and to the strongly correlated non-adiabatic coupling.

[d] E-mail: daniel.borgis@univ-evry.fr, fax: (33)-1-69-47-01-46
rossky@mail.utexas.edu, fax: (1)-512-471-3555
turi@chem.elte.hu, fax: (36)-1-372-2592.

I. Introduction

The importance of non-adiabatic (NA) relaxation in condensed phase physics and chemistry has attracted significant scientific attention in the last decades. With the rapid advance of theoretical methodologies and experimental techniques, it has become possible to gain insight into the microscopic nature of NA processes, of which proton and electron transfer, vibrational relaxation, and intermolecular energy redistribution are the most prominent examples.[1]

In most computational treatments, liquid phase NA processes are modeled by mixed quantum-classical simulation techniques. In mixed quantum-classical methods, one describes a limited number of physically relevant degrees of freedom quantum mechanically, while the rest, the bath, is treated classically.[2-9] In practice, the calculation of NA decay rates is generally based on the time-dependent perturbation theory. The most straightforward approach employs the Fermi golden rule to compute the NA decay rate from the simulated adiabatic Born-Oppenheimer dynamics.[5,6,10] The great advantage of using the Fermi golden rule is that, beyond its simple form, it expresses the transition rate in terms of a time correlation function (TCF).

In fact, the TCF formalism is a very effective tool in investigating various problems of statistical mechanics, in particular, phenomena in condensed phases.[11-22] It is well known that, while classical TCF's can be employed safely only in those systems where quantum effects are negligible, the computation of full quantum mechanical TCF's is still out of reach for systems with a large number of degrees of freedom. This poses a serious obstacle, since one has to resort to predicting the full quantum TCF's from the classical or mixed quantum-classical analogs. A possible approximate route to circumvent the quantum many-body problem, an *a posteriori* quantization of classical TCF's, has been recognized, and several

approximate quantization schemes have been proposed in the literature.[13-19] Although, it has become clear that the general solution of the problem is unlikely, and the applicability of various approximation schemes may be limited to specific problems, the method is still of great scientific interest.[18-22] In particular, the key issue is the critical application of the approximations to well-chosen, well-defined physical problems. Several other related approaches have been developed in the literature, of which we mention the dispersed polaron/spin-Boson Hamiltonian approach for evaluating the rate constant for electron transfer and related processes.[23-25]

In this study, we propose a new, alternative form of the Fermi golden rule, in terms of quantum TCF's, which is valid for a generic NA two-state process in condensed phase and is amenable to an *a posteriori* quantization of classically determined TCF's. The formalism will be subsequently applied to the problem of the electronic relaxation of an equilibrated excited state solvated electron. The relaxation phenomena in solvated electron systems, the NA decay, and the subsequent solvent relaxation, are the direct reflection of the underlying strong solute-solvent coupling. For this reason the solvated electron has been considered as a sensitive probe and model of solvation dynamics, and has been the subject of several theoretical[3,5-10,26-51] and experimental studies.[52-63] Within our modified golden rule formula, we wish to calculate the classical decay rates, and compare them to the quantum transition rate obtained by quantizing the classical TCF's. This comparison may shed light on the contributions of the different nuclear modes, and clarify the applicability of the presently employed quantization schemes to the solvated electron relaxation problem. The comparison of the classical and quantum rates makes it also possible to characterize decoherence, a recurring issue in mixed quantum-classical approaches.[38-41,51,64,65] For this problem, we will follow closely the Prezhdo-Rossky treatment of decoherence.[40]

We consider two solvents, water and methanol, in the present study. For water, the interpretation of pump-probe experiments in terms of solvent reorganization dynamics and/or excited state population decay is still a controversial issue. The NA decay times inferred from experiments range presently from 50 to ~1000 fs. According to an early scenario proposed by the Barbara group,[55,56] the NA decay of the excited state occurs within ~200 fs and is followed by a ~1 ps relaxation of the ground state. Their later experiments were interpreted in terms of a ~300 fs solvent relaxation in the 2p-excited state followed by a NA decay with a time constant around 1 ps.[57,58] More recent work by Assel *et al.*,[59,60] supported the former scenario. Very recently Pshenichnikov *et al.*[61] have performed photon-echo experiments with very short (5 fs) pulses and they have concluded that the p-state lifetime should be much shorter than stated before, ~50 fs, with an (expected) $\sqrt{2}$ kinetic isotope effect in heavy water. From theoretical point of view, the results are also quite scattered and the determination of NA decay rates from MD simulations seems to depend drastically on the water model, the electron-water pseudopotential, and the level of quantum simulation methodology employed. Using a golden rule approach with an equilibrated excited state trajectory, and with a rigid, polarizable water model, Staib and Borgis obtained a NA decay time of ~300 fs,[6] whereas, with a similar approach but with a different flexible water model and incorporation of nuclear semi-classical (high-temperature) corrections, Neria and Nitzan predicted ~220 fs.[5,10] Schwartz and Rossky have performed direct non-adiabatic simulations of an electron excited from its ground state to one of the p-states and they have monitored the subsequent relaxation, including solvent reorganization and surface hopping to the initial electronic state. Although their approach intermixes the two effects, they were able to extract an averaged p-state lifetime of 700 fs and they proposed an extrapolated lifetime of 450 fs for an equilibrated p-state.[34,35]

For methanol, no evident controversy seems present, but it must be noticed that experiments[62,63] and simulations[47-51] are less plethoric. The transient hole-burning experiments of Barbara *et al.* suggest a $p \rightarrow s$ non-adiabatic decay of ~500 fs followed by an order of magnitude slower ground state solvation.[63] From their non-adiabatic MD simulations, Mináry *et al.* predicted an equilibrated p-state survival time of ~660 fs, and they found also that, on average, the excited state solvation is complete by the time the electronic transition occurs.[50] This means that computing the decay rate independently, from an equilibrated excited state trajectory, is legitimate, and the overall relaxation process can be thought of as a three-step process, excited state solvent relaxation first, followed by non-adiabatic transition, and then ground state relaxation. The present work will focus mainly on the second step.

The structure of the paper is as follows. In Sec. II we derive an alternative form of the full, quantum mechanical golden rule expression which is especially suitable for the application of the TCF formalism. Starting from the classical form of the golden rule expression we examine the harmonic quantization scheme[17,18] in more detail, as well as the standard quantization[15,16] for comparison. Sec. III shows and discusses the numerical results of our mixed quantum-classical simulations for a solvated electron in water and methanol in connection to available theoretical and experimental predictions. Evaluation of the classical and quantized rates is performed in time-domain and in frequency-domain formulation. We also point out a close connection of our formalism and decoherence. Sec. IV concludes the paper.

II. Fermi Golden Rule Expression for Non-Adiabatic Electronic Transitions

The golden rule expression for the thermal transition rate between two adiabatic electronic states, 1 and 2, may be written in a time-dependent form[5,10,40]

$$k_{1\to 2} = \frac{1}{\hbar^2}\int_{-\infty}^{\infty} dt \left\langle e^{iH_1 t/\hbar}\langle 1|V|2\rangle e^{-iH_2 t/\hbar}\langle 2|V|1\rangle \right\rangle_T = \frac{1}{\hbar^2}\int_{-\infty}^{\infty} dt \mathrm{Tr}\left(\left[e^{iH_1 t/\hbar}\langle 1|V|2\rangle e^{-iH_2 t/\hbar}\langle 2|V|1\rangle\right]\rho_T\right)$$
$$= \frac{1}{\hbar^2}\int_{-\infty}^{\infty} dt \left[\frac{1}{Z_1}\frac{1}{\hbar^2}\sum_i e^{-\beta E_{1i}}\langle i|e^{iH_1 t/\hbar}\langle 1|V|2\rangle e^{-iH_2 t/\hbar}\langle 2|V|1\rangle|i\rangle\right] \tag{1}$$

where H_1 and H_2 are the nuclear Hamiltonians corresponding to the first and second adiabatic electronic states, $|1\rangle$ and $|2\rangle$, V is the non-adiabatic coupling operator resulting from the nuclear kinetic energy, and ρ_T is the canonical density operator for the thermal equilibrium of the nuclear modes, *i*, on the initial electronic surface

$$\rho_T = \frac{1}{Z_1}\sum_i e^{-\beta E_{1i}}|i\rangle\langle i|, \tag{2}$$

with $Z_1 = \mathrm{Tr}(e^{-\beta H_1})$, the canonical partition function. In the following, for the sake of compactness, we will adopt the $\langle ... \rangle$ notation for thermal averaging (tracing) over the initial (nuclear) distribution.

According to the usual procedure,[10,11,20,40] the coupling matrix elements are approximated by neglecting the second derivatives of the electronic wavefunction with respect to the nuclear coordinates,

$$\langle 1|V|2\rangle = \sum_\alpha \langle 1|P_\alpha|2\rangle P_\alpha = \sum_\alpha S_\alpha P_\alpha\,, \tag{3}$$

where P_α are the conjugate momenta of the nuclear mode α.

Staib and Borgis introduced an alternative form for the NA transition rate writing[6]

$$k_{1\to 2} = \frac{1}{\hbar^2}\int_{-\infty}^{\infty} dt \left\langle V_{12}(t)\exp_{(+)}\left[\frac{i}{\hbar}\int_0^t \Delta H_{12}(\tau)d\tau\right]V_{21}(0)\right\rangle, \tag{4}$$

where $\exp_{(+)}$ is the time-ordered exponential, and $\Delta H_{12}(\tau)$ and $V_{12}(t)$ are defined as

$$\Delta H_{12}(\tau) = e^{iH_1\tau/\hbar}(H_1 - H_2)e^{-iH_1\tau/\hbar}, \tag{5}$$

and

$$V_{12}(t) = e^{iH_1 t/\hbar}\langle 1|V|2\rangle e^{-iH_1 t/\hbar}. \tag{6}$$

Note, that the dynamics involved occurs on the initial adiabatic surface with Hamiltonian H_1. Eq. (4) will serve as a starting point to derive another useful form of the golden rule. First, we use the following simple relation to bring an operator, *A*, to exponential form:

$$A = \lim_{\lambda\to 0}\frac{\mathrm{d}}{\mathrm{d}\lambda}e^{\lambda A}. \tag{7}$$

Application of Eq. (7) in the golden rule formula of Eq. (4) leads to

$$k_{1\to 2} = \frac{1}{\hbar^2}\int_{-\infty}^{\infty} dt\left\{\lim_{\lambda_t\to 0}\frac{\mathrm{d}}{\mathrm{d}\lambda_t}\left\{\lim_{\lambda_0\to 0}\frac{\mathrm{d}}{\mathrm{d}\lambda_0}\left\langle e^{\lambda_t V_{12}(t)}\exp_{(+)}\left[\frac{i}{\hbar}\int_0^t \Delta H_{12}(\tau)d\tau\right]e^{\lambda_0 V_{21}(0)}\right\rangle\right\}\right\}. \tag{8}$$

In the evaluation of Eq. (8), we successively employ the cumulant expansion of the exponentials including the cumulant expansion of the time ordered exponential to second order, and assume that the order of differentiation with respect to λ and tracing over the initial nuclear conditions can be exchanged. The procedure is similar in spirit to that of Nitzan and Silbey for the relaxation in simple quantum systems.[66] The final form of the golden rule reads now as

$$\begin{aligned} k_{1\to 2} = \frac{1}{\hbar^2}\int_{-\infty}^{\infty} dt\Bigg[& e^{i\langle\Omega_{12}(t)\rangle t}\times\exp\left\{-\int_0^t d\tau_1\int_0^{\tau_1} d\tau_2\langle\delta\Omega_{12}(\tau_2)\delta\Omega_{12}(0)\rangle\right\}\times\Big\{\langle V_{12}(t)V_{21}(0)\rangle \\ & + i\langle V_{12}\rangle\int_0^t \mathrm{d}\tau\langle\delta\Omega_{12}(\tau)\delta V_{21}(0)\rangle + i\langle V_{21}\rangle\int_0^t \mathrm{d}\tau\langle\delta V_{12}(\tau)\delta\Omega_{12}(0)\rangle \\ & - \int_0^t \mathrm{d}\tau_1\int_0^t \mathrm{d}\tau_2\langle\delta V_{12}(\tau_1)\delta\Omega_{12}(0)\rangle\times\langle\delta\Omega_{12}(\tau_2)\delta V_{21}(0)\rangle\Big\}\Bigg], \end{aligned} \tag{9}$$

where we introduced $\Omega_{12}(t) = \Delta H_{12}(\tau)/\hbar$, and δ stands for the fluctuations from the averages. With the expression of the coupling in Eq. (3), and noting that the momentum P_α is

odd in time, one can infer that the thermal average of the coupling matrix disappears. Consequently, we write for the quantum transition rate

$$k_{1\to 2} = \frac{1}{\hbar^2}\int_{-\infty}^{\infty} dt\Bigg[e^{i\langle \Omega_{12}(t)\rangle t} \times \exp\Bigg\{-\int_0^t d\tau_1 \int_0^{\tau_1} d\tau_2 \left\langle \delta\Omega_{12}(\tau_2)\delta\Omega_{12}(0)\right\rangle\Bigg\} \times \Bigg\{\left\langle V_{12}(t)V_{21}(0)\right\rangle - \int_0^t \mathrm{d}\tau_1 \int_0^t \mathrm{d}\tau_2 \left\langle V_{12}(\tau_1)\Omega_{12}(0)\right\rangle \times \left\langle \Omega_{12}(\tau_2)V_{21}(0)\right\rangle\Bigg\}\Bigg] \tag{10}$$

Eq. (10), and the more general Eq. (9) represent two of the main results of the present paper. They provide fully quantum mechanical expressions for the transition rate using the cumulant expansion of the exponential operators up to second order as the only approximation beyond the original Fermi golden rule first order perturbation treatment. Note, that the great advantage of the above expressions is that they do not contain time-ordered exponentials, and that only thermal correlation functions for the relevant quantities appear in the transition rate.

Despite the relatively simple form of the golden rule transition rate of Eq. (10), its application may still be cumbersome in practical applications mainly due to the difficulty of the evaluation of the quantum correlation functions. An attractive approach is to replace the quantum correlation functions by their classical counterparts computed from mixed quantum-classical molecular dynamics simulations. The evaluation of the classical correlation functions is straightforward: $\Omega_{12}^{cl}(t) = (E_1 - E_2)/\hbar$ is simply the energy gap of the quantum subsystem submerged in the classical bath. The transition rate, thus, simplifies in the classical limit to

$$k_{1\to 2}^{cl} = \frac{1}{\hbar^2}\int_{-\infty}^{\infty} dt e^{i\left\langle \Omega_{12}^{cl}(t)\right\rangle t} \times \exp\Bigg\{-\int_0^t d\tau_1 \int_0^{\tau_1} d\tau_2 \left\langle \delta\Omega_{12}^{cl}(\tau_2)\delta\Omega_{12}^{cl}(0)\right\rangle\Bigg\} \times \Bigg\{\left\langle V_{12}^{cl}(t)V_{21}^{cl}(0)\right\rangle - \int_0^t \mathrm{d}\tau_1 \int_0^t \mathrm{d}\tau_2 \left\langle V_{12}^{cl}(\tau_1)\times\Omega_{12}^{cl}(0)\right\rangle \times \left\langle \Omega_{12}^{cl}(\tau_2)\times V_{21}^{cl}(0)\right\rangle\Bigg\}, \tag{11}$$

where the quantum thermal averaging is replaced for classical averaging.

The rate can also be expressed in a more condensed form as[5,10]

$$k_{1\to 2} = \int_0^\infty dt K(t)\,, \tag{12}$$

where $K(t)$ represents the real part of the integrand in Eq. (10) multiplied by $2/\hbar^2$. This quantity can be interpreted, in a Kubo sense, as the "chemical flux" correlation function associated to the transport coefficient constituted by the chemical rate.[67-69]

In the remaining of the paper, for convenience, we drop the *cl* superscripts for the classical quantities. Instead, the quantum quantities will be denoted by a *q* index. To facilitate further discussion we can introduce the following (normalized and unnormalized) classical correlation functions:

$$\tilde{C}_\Omega(t) = \left\langle \delta\Omega_{12}(t)\delta\Omega_{12}(0)\right\rangle / \left\langle \delta\Omega_{12}^2\right\rangle, \tag{13}$$

$$C_\Omega(t) = \left\langle \delta\Omega_{12}(t)\delta\Omega_{12}(0)\right\rangle, \tag{14}$$

$$C_V(t) = \left\langle V_{12}(t)V_{12}(0)\right\rangle, \tag{15}$$

$$C_{V\Omega}(t) = \left\langle V_{12}(t)\Omega_{12}(0)\right\rangle. \tag{16}$$

In the classical case, the time dependent flux then reads

$$K(t) = \frac{2}{\hbar^2}\left[C_V(t) - \left(\int_0^t d\tau C_{V\Omega}(\tau)\right)^2\right] G(t)\cos(\left\langle \Omega_{12}\right\rangle t)\,, \tag{17}$$

where $G(t)$ is the "dephasing function" defined by

$$G(t) = \exp\left\{ -\int_0^t d\tau_1 \int_0^{\tau_1} d\tau_2 C_\Omega(\tau_2)\right\} = \exp\left\{ -\left\langle \delta\Omega_{12}^2\right\rangle \int_0^t d\tau_1 \int_0^{\tau_1} d\tau_2 \tilde{C}_\Omega(\tau_2)\right\}, \tag{18}$$

and, in reference to the theory of band shapes in condensed phases,[12] $\tau_\phi = \left\langle \delta\Omega_{12}^2\right\rangle^{-1/2}$ defines the classical dephasing time.

The transition rate calculated from classical correlation functions, however, may differ significantly, even by several orders of magnitude, from the quantum rate as was illustrated

by studies of Berne and his co-workers.[18,20,21] These authors also point out that the classical limit of Eq. (10) is not uniquely defined, with dynamics taking place on the average of the initial and final potential surfaces provide the most accurate result in cases examined.[20] *A posteriori* quantization schemes of the classical correlation functions, that have been introduced mostly in a spectroscopic context,[13-19] provide an effective way to include quantum effects. They have been reviewed and tested recently for simple analytical examples[19] and for vibrational relaxation in liquids.[22] The so-called harmonic quantization scheme assumes linear coupling of the quantum subsystem to a bath of linearly coupled harmonic oscillators.[17,18] In that case, the quantized version of a classical correlation function $C(t) = \langle A(t)A(0) \rangle$ is written in the frequency domain as

$$\hat{C}^q(\omega) = \frac{\beta\hbar\omega}{2\tanh(\beta\hbar\omega/2)} \times \frac{2}{1+e^{-\beta\hbar\omega}} \hat{C}(\omega) = \frac{\beta\hbar\omega}{1-e^{-\beta\hbar\omega}} \hat{C}(\omega), \qquad (19)$$

where $\hat{C}(\omega)$ is the Fourier transform of the classical correlation function $C(t)$, $\hat{C}^q(\omega)$ is the quantized correlation function in the frequency domain, and $\beta = 1/kT$. In the first equality, the first term accounts for the renormalization of the individual modes amplitude when going from the classical to the quantum regime, whereas the second one accounts for the detailed balance condition fulfilled by quantum correlation functions, $\hat{C}^q(-\omega) = e^{-\beta\hbar\omega}\hat{C}^q(\omega)$. This formula transforms in the time domain to

$$C^q(t) = \int_0^\infty d\omega \frac{\hat{C}(\omega)}{\pi} \frac{\beta\hbar\omega}{2} (\coth(\beta\hbar\omega/2)\cos(\omega t) - i\sin(\omega t)). \qquad (20)$$

Another well-known quantization method, the standard quantization scheme,[15,16] which retains only the second multiplication factor of the first equality of Eq. (19), transforms to a similar expression:

$$C^q(t) = \int_0^\infty d\omega \frac{\hat{C}(\omega)}{\pi} \tanh(\beta\hbar\omega/2)(\coth(\beta\hbar\omega/2)\cos(\omega t) - i\sin(\omega t)). \qquad (21)$$

The standard quantization, thus, accounts only for the detailed balance condition, but neglects the renormalization of the individual mode amplitudes. Several other quantization schemes have also been proposed in the literature, of which we can mention the Schofield,[13] the Egelstaff,[14] and the Kim-Rossky scheme.[19] Since we believe that the electronic relaxation is predominantly coupled to the vibrational modes of the classical bath, it is the harmonic scheme which we examine in more detail in the present work. For comparison we also evaluate the rates with the standard quantization scheme.

If the harmonic quantization is chosen for $C_\Omega(t)$, $C_V(t)$ and $C_{V\Omega}(t)$, and if one defines the spectral density of $C(t)$ as $J(\omega) = \hat{C}(\omega)/\pi$, then one finds the following formula for the quantum transition rate, similar to the one derived by Kubo and Toyozawa,[11] and Egorov *et al.*,[20] in terms of $J_\Omega(\omega)$, $J_V(\omega)$, $J_{V\Omega}(\omega)$ as

$$k_{1\to 2} = \frac{1}{\hbar^2}\int_{-\infty}^{\infty} dt e^{i\langle\Omega_{12}^{cl}\rangle t} \times \exp\left\{\int_0^\infty d\omega J_\Omega(\omega)\frac{\beta\hbar}{2\omega}\left(\coth(\beta\hbar\omega/2)(\cos(\omega t)-1)+i(\omega t-\sin(\omega t))\right)\right\}$$
$$\times\left\{\int_0^\infty d\omega\, J_V(\omega)\frac{\beta\hbar\omega}{2}\left(\coth(\beta\hbar\omega/2)\cos(\omega t)-i\sin(\omega t)\right)\right.$$
$$\left.+\left(\int_0^\infty d\omega\, J_{V\Omega}(\omega)\frac{\beta\hbar}{2}\left(\coth(\beta\hbar\omega/2)\left(\cos(\omega t)-1\right)-i\sin(\omega t)\right)\right)^2\right\} \quad . \tag{22}$$

At this point, we note, that following similar work,[11,20,40] we further simplified the coupling matrix elements in Eq. (22), by assuming that the S_α terms (see Eq. (3)) are basically independent of the nuclear coordinates. The general expression of Eq. (22) relates to the formula discussed by Egorov *et al.*,[20] for the particular case of a two-state system linearly coupled to a bath of harmonic oscillators in the Born-Oppenheimer linear diagonal coupling case. The relation of the formulas can be easily proved by using the Hamiltonian of Ref 20 and the exact classical spectral densities for the correlation functions of Eq. (22). We, however, note a minor difference in the expressions for the last term of Eq. (22), (which

appears as modulo square in the work of Berne and his co-workers) and is the consequence of the application of the cumulant expansion to the time-ordered exponential.

Eq. (22) illustrates two important points. First, one finds that Eqs (9) and (10) closely reproduce the quantum mechanical result of a simple, analytically solvable model. This illustrates the applicability of the modified golden rule formula. Perhaps this is not surprising considering that the approach is exact for constant coupling, and coupling linear in coordinate space. The fact that it gives results that are similar (not completely identical) to the exact analytical results discussed in Ref 20 for a coupling linear in momentum space is a good indication that the approximation remains reasonable beyond its domain of exact application. For more general couplings, one certainly has to rely on the general applicability of a second-order cumulant expansion which has proved its accuracy in many instances beyond the linear coupling/harmonic bath case. On the other hand, it is also evident, that the application of the classical transition rate with the harmonic correction scheme (Eqs (20) and (22)) yields the identical transition rate derived from Eqs (9) and (10) for the same analytically solvable model. This finding is our main motive to use the harmonic correction scheme in the present study. Nevertheless, in order for Eq. (22) to be applicable for a particular problem, the two basic assumptions must be satisfied, namely, that the S_α terms are nearly independent of the nuclear coordinates, and that the nuclear modes coupled to the quantum subsystem are predominantly harmonic. In our investigated model, electronic relaxation of an excited state solvated electron in water and methanol, both approximations appear to hold well.

III. Application to a solvated electron in water and methanol

A. Motivations

As stated in the introduction, the solvated electron has been the subject of intensive work in the past two decades. First, as the simplest quantum mechanical solute which can be conceived, it constitutes an ideal probe for solvation dynamics since no internal energy redistribution has to be considered. It is also perfectly suited to quantum/classical molecular dynamics simulations so that ultrafast time-resolved spectroscopy and theoretical predictions can be confronted. From a computational point of view, there are two ways to envision the problem. One route is to directly mimick the experiments on the computer and study the non-adiabatic dynamics of the electron from a prepared excited electronic state via non-adiabatic simulation techniques. Another way, familiar in spectroscopy is to interpret the experimental signal in terms of bath dynamics (T_2) and population relaxation (T_1) times. Those times can be computed from MD simulations using linear response theory and the suitable Green-Kubo relation relating the observable quantity to the time integral of an associated correlation function. In this perspective, the solvation dynamics time can be related to the energy gap autocorrelation function in either the ground or excited state. The population decay rate can be obtained from the time dependent formulation of the Fermi golden rule developed in the previous section, where it was defined as the time integral of a "chemical flux" correlation function; see Eqs (10)-(12). Compared to direct non-adiabatic simulations, the correlation function approach has a number of potential weaknesses, in particular the validity of linear response for solvation dynamics and of first order perturbation theory for the population decay rates. Furthermore, solvent reorganization and electronic relaxation can be intertwined rather than well separated phenomena. On the other hand, if the separation is justified, the theoretical expression of the third-order time-dependent pump-probe signal, involving, in general, a 4-time correlation function, reduces to a simpler expression involving the two-time correlation function of the energy gap and the non-adiabatic decay rates.[44,70] These considerations motivate the present work.

B. Simulation results

To compute the non-adiabatic decay from an excited p-state to an s-type ground state hydrated electron, we have performed adiabatic mixed quantum-classical molecular dynamics simulations of an excited state electron embedded in a classical water bath. The basics of the method can be found in Ref. 7. The details of the actual simulations are similar to our previous simulations in Ref. 46. The solvent bath consists of 1600 water molecules in a cubic simulation cell. The molecular interactions are described by three-site classical model potentials with added internal flexibility. The electron is treated quantum mechanically in a plane wave basis represented on 16^3 gridpoints equidistantly distributed in a box, with the edge length equal to half of the length of the simulation cell. The interaction between the quantum particle and the classical molecules is modeled by a pseudopotential.[46] The nuclear configurations are adiabatically propagated on the potential surfaces using the sum of classical and Hellmann-Feynman forces. The simulation time step is 1 fs. The long-range part of the interactions and the forces are calculated using the Ewald summation technique including solvent-solvent and the solvent-electron interactions explicitly, similar to the work of Rossky and co-workers.[42] We note, that it turns out to be quite difficult to generate lengthy stable equilibrium adiabatic excited state trajectories in the solvated electron systems; instability is signified by an unphysical collapse of the energy gap. Nevertheless, it is clear, that it is not the model that is at fault, but the accumulation of numerical errors that appears to cause the problem. For this reason, in the present work, we *illustrate* the use and consequences of the formalism introduced in Sec. II for a relatively short but stable, 20 ps long excited state hydrated electron trajectory.

We have also considered results obtained from a stable 20 ps equilibrium excited state trajectory portion of a previous methanol simulation. The details of generating that trajectory

are very similar to those above, and are described in detail in Ref 51. We note, that in the methanol case the simulation box contained only 200 molecules, and we employed the modified pseudopotential of Zhu and Cukier.[47,48]

In Figure 1, we display the time dependent frequency gap, $\Omega_{12}(t)$, and the time-dependent non-adiabatic coupling, $V_{12}(t)/\hbar$, for water and methanol. Perturbation theory treatment of a non-adiabatic decay rate requires that the non-adiabatic condition $\lambda = \frac{|V_{12}(t)|}{\Omega_{12}(t)} << 1$ is fulfilled. It can be verified visually on the trajectories that this condition is generally fulfilled, with only rare (<1%) periods of time when the coupling magnitude exceeds the energy gap. Hence, both the water and methanol simulations appear well within the perturbative regime, $\langle\lambda\rangle << 1$, and one finds along the trajectories that $\langle\lambda\rangle \cong 0.10$. Thus, we believe, the application of a perturbative approach to the water and methanol trajectories is well justified.

For the present models, the average energy gap turns out to be larger in water than methanol, $\langle H_{12}\rangle$ = 431 meV and $\langle H_{12}\rangle$= 275 meV, respectively corresponding to $\langle\Omega_{12}\rangle$= 0.65 fs^{-1} and $\langle\Omega_{12}\rangle$= 0.42 fs^{-1}. The smaller energy gap for the present (Turi-Borgis) pseudopotential[46] relative to the Schnittker-Rossky pseudopotential (0.8 eV)[32,42] can be attributed to the fact that the Turi-Borgis pseudopotential is both softer and finite at the oxygen origin.[46] Note also, that, for methanol, the ground-state absorption spectrum computed with the pseudopotential of Zhu and Cukier is red-shifted relative to the experiment. A corresponding deficiency may carry over to the equilibrium excited state.[48] In both solvents, as expected based on the discussion in Sec. II, the computed average coupling, $\langle V_{12}\rangle$, is virtually zero. The different values found for the energy gap and the non-adiabatic coupling

are summarized in Table I for the two cases. Note, that the classical dephasing times $\tau_\phi = \left\langle \delta\Omega_{12}^2 \right\rangle^{-1/2}$ are very small in both solvents, around 5 fs.

The normalized energy gap correlation function for methanol and water are displayed in Figure 2. For water, the fast initial Gaussian part with a characteristic time of ~10 fs accounts for about 30% of the overall decay. The longer time decay occurs with a single exponential of ~700 fs characteristic time. Similarity of the present numbers to those obtained previously from the ground state equilibrium simulation indicates that the linear response theory holds well for the model.[46] In the case of methanol, the initial Gaussian decay has a much smaller amplitude, and the overall decay is slower than for water. This fact has already been recognized for both the ground and excited state electrons,[49] and it is a reflection of the slower overall rotational reorganization in methanol. Nevertheless, one can readily notice that for the correlation functions in water and methanol even the fastest decay takes place on a timescale which is longer than the dephasing time τ_Φ, so that the "homogeneous broadening" limit will apply to the thermal rate expressions.

The normalized coupling autocorrelation function, $C_V(t)$, and the coupling-frequency gap cross correlation function, $C_{V\Omega}(t)$, appear highly oscillatory and are best represented directly by their spectral densities. In Fig. 3 we show the coupling spectral density defined previously as $J_V(\omega) = \hat{C}_V(\omega)/\pi$ for water, and methanol. It is clear that the coupling fluctuations are entirely driven by the solvent vibrations. In both spectra, one can clearly distinguish the librational, bending, and O-H stretching modes. Further, these vibrational mode coupling amplitudes typically appear considerably blue-shifted with respect to the bulk vibrational density of states. This is an indication of the intensity of the interaction between the excited state electronic wave function and the nearest solvent molecules' vibrations. These results are in accord with previous analysis of Prezhdo and Rossky.[37]

C. Classical rates

Using the various computed correlation functions, we can directly generate the classical flux correlation function $K(t)$ of Eq. (17). The calculated functions are displayed in Fig. 4 for water and methanol. It can be seen that $K(t)$ decays on an extremely fast timescale of a few femtoseconds. On this short timescale it appears that two simplifications can be made safely for the evaluation of the rate. First, the cross correlation term is, for short times, $\mathrm{O}(t^4)$ and can be neglected. Thus, $K(t)$ simplifies to

$$K(t) = \frac{2}{\hbar^2} C_V(t)\, G(t) \cos(\langle \Omega_{12} \rangle t) . \tag{23}$$

This decorrelation approximation between coupling and energy gap was postulated in Ref. 6 and is fully justified here. Furthermore, since solvent dynamics occurs on a slower timescale, the exponential function $G(t)$ can be replaced by a Gaussian function, leading to

$$K(t) = \frac{2}{\hbar^2} C_V(t)\, e^{-\frac{1}{2}\langle \delta\Omega_{12}^2 \rangle t^2} \cos(\langle \Omega_{12} \rangle t) . \tag{24}$$

The complete (Eq. (17)) and approximated (Eq. (24)) flux correlation functions are compared in Fig. 4. Clearly, they are undistinguishable on the scale of the figure so that Eq. (24) provides a very good (and simple) approximation. Then, the chemical flux function, $K(t)$, can be integrated in time according to Eq. (12) to provide the classical rate and the associated non-adiabatic transition time $\tau_{1\to 2} = k_{1\to 2}^{-1}$.

We find $\tau_{1\to 2} = 60$ fs for water, and $\tau_{1\to 2} = 160$ fs for methanol. In both cases, this is much shorter than previous estimates also based on classical nuclear dynamics. Various reasons can be invoked for explaining this discrepancy. For water, the calculations of Staib and Borgis are the easiest to reason since those authors used a rigid water model, with no consideration of the intramolecular vibrational mode contributions,[6] and it appears clear from

the coupling spectral density in figure 3 that this approach misses the dominant effect. It is possible to include the vibrational contributions in this rigid-water scheme by using a normal coordinate Taylor expansion of the electronic coupling around the water rigid geometry.[71] This procedure leads to conclusions which are close to those described in this paper. Neria and Nitzan, employing a Fermi golden rule approach similar to the one proposed here with a high temperature approximation to quantization of the nuclear dynamics,[5,10] found a 220 fs lifetime. We can easily attribute this discrepancy to different electron-water pseudopotentials and the different water models. The rate is most sensitive to both the initial value of the coupling, $\langle V_{12}^2 \rangle$, and the average electronic frequency gap, $\langle \Omega_{12} \rangle$. These quantities do differ from one model to the other, and their influence on the computed rate will be discussed in more detail later in this paper.

The simulations of Schwartz and Rossky with the same water model and different pseudopotential[32] resulted in much longer lifetimes in the half-picosecond range.[34-36] These authors, however, have not applied an equilibrium golden rule, but, rather, performed non-equilibrium non-adiabatic simulations, exciting an equilibrium ground state electron at time zero for a specific excitation wavelength and monitoring the subsequent solvation dynamics and non-adiabatic events. An estimated equilibrated p-electron decay rate is extracted from an extrapolation formula based on the observed survival times. For water, Schwartz and Rossky found that, on average, the radiationless transition occurs after the major part of the solvation dynamics is completed.[34] Similar conlusions were drawn from non-adiabatic electronic relaxation trajectories in methanol by Mináry *et al.*[50] These observations favour the possibility of decoupling the two types of entangled events. It might, however, also be true that our finding of a shorter lifetime for an *equilibrated* p-electron reflects the interdependency between solvation dynamics, spectral diffusion and electronic transition in the non-adiabatic dynamics. Before proceeding further in this discussion, it seems judicious to examine the

nuclear quantum effects on the transition rate. It is one advantage of the time correlation function approach that it allows for an easy incorporation of the quantum character of nuclear motions. We illustrate these considerations below.

D. Quantized correlation functions and quantum transition rates: Time domain formulation

For the procedure to compute the quantum corrections to the classical rate, we use the calculated classical spectral densities, in particular the one displayed in figure 3, and apply them in the time-dependent formula of Eq. (22). Integration of the equation in time results in the quantized rate. Note again, that this formula is based on the so-called harmonic quantization procedure which is likely to be valid here since the coupling to the bath occurs predominantly through the vibrational modes. For comparison, the standard[15,16] quantization scheme will also be considered. The (normalized) quantized chemical flux correlation function $K^q(t)$ is plotted in Fig. 5, and can be compared to the classical one. Again, the two approximations discussed previously, the neglect of the cross-correlation contribution, and the Gaussian approximation for the quantized dephasing function $G^q(t)$, can be tested, yielding a simplified expression of $K^q(t)$

$$K^q(t) = \mathrm{Re}\left[e^{i\langle\Omega_{12}\rangle t}\; e^{-\frac{1}{2}\left\langle \delta\Omega_{12}^2 \right\rangle_q t^2} \int_0^\infty d\omega\, J_V(\omega) \frac{\beta\hbar\omega}{2} \left(\coth\left(\beta\hbar\omega/2\right)\cos\left(\omega t\right) - i\sin\left(\omega t\right)\right)\right] \tag{25}$$

where the quantized frequency gap fluctuation is defined by

$$\left\langle \delta\Omega_{12}^2 \right\rangle_q = \left\langle \delta\Omega_{12}^2 \right\rangle \int_0^\infty d\omega \tilde{J}_\Omega(\omega)\, \frac{\beta\hbar\omega}{2} \coth\left(\frac{\beta\hbar\omega}{2}\right). \tag{26}$$

In Eq. (26) $\tilde{J}(\omega) = \tilde{C}_\Omega(\omega)/\pi$ is the spectral density of the normalized classical energy gap fluctuation autocorrelation function. Eqs (25) and (26) provide an excellent approximation to

the quantized classical flux correlation function (see Fig. 5). Interestingly, the computed quantized frequency gap fluctuations are increased only slightly relative to the classical counterparts. However, the values of the mean square of the coupling, $\left\langle V_{12}^2 \right\rangle_q$, are a factor of approximately 6-8 times greater than the classical values (see Table I), implying a significant increase of the quantized rates.

The quantized rate can be obtained by direct numerical integration of Eq. (12). The non-adiabatic transition times (classical and quantized) are summarized in Table II. With the application of the harmonic quantization scheme we find $\tau_{1\to 2}^q = 4.0$ fs for water, and $\tau_{1\to 2}^q = 17$ fs for methanol, respectively. There are (at least) two points to emphasize here. First, the quantum effects appear indeed very important, with roughly an order of magnitude between the classical and quantum answers. This fact can be expected since, as illustrated in Fig. 3, the coupling fluctuations are entirely dominated by the relatively high frequency solvent vibrational modes. The intensity of these modes (and of the associated velocities which appear in the non-adiabatic coupling V_{12}) are multiplied by a factor $\frac{\beta\hbar\omega}{2\tanh(\beta\hbar\omega/2)}$ when going from the classical to the quantum limit. The second observation is that the quantum effects somehow overemphasize the conclusion already found in the classical case. We find that the lifetime of an equilibrated p-state in both methanol and water is extremely short, and, at the timescale of a pump-probe experiment, it could be even considered as "instantaneous". The standard quantization scheme provides a somewhat slower relaxation, with $\tau_{1\to 2}^q = 30$ fs, and $\tau_{1\to 2}^q = 80$ fs, for water and methanol, respectively, but still predicts exceedingly fast rates. We will come back to the implication of these findings for the interpretation of pump-probe experiments below. Before that discussion, however, we find it instructive to discuss the quantum dephasing function $G^q(t)$, and make a connection to the decoherence time

formalism introduced by Rossky and collaborators.[38-41,51] We then look at the quantum rates from a different perspective, in the frequency rather than time domain.

E. Quantized correlation functions and quantum transition rates: Decoherence

Let us define a Gaussian decoherence function similar in spirit to that of Prezhdo and Rossky[40] as $D(t) = G^q(t)/G(t)$, accounting for the nuclear quantum effects in the energy gap correlation function. Thus, we are lead to the following expression for the decoherence function

$$D(t) = e^{-\frac{t^2}{2\tau_d^2}} = e^{-\frac{1}{2}\left(\left\langle \delta\Omega_{12}^2 \right\rangle_q - \left\langle \delta\Omega_{12}^2 \right\rangle\right)t^2} , \tag{27}$$

where τ_d defines the decoherence time as

$$\tau_d = \left(\left\langle \delta\Omega_{12}^2 \right\rangle \int_0^\infty d\omega\, \tilde{J}_\Omega(\omega) \left(\frac{\beta\hbar\omega}{2} \coth\left(\frac{\beta\hbar\omega}{2} \right) - 1 \right) \right)^{-1/2} \tag{28}$$

in the harmonic quantization scheme. In the high temperature limit of the frozen Gaussian wave packet formulation[5,10,40,51] each normal mode (or each atom) is represented by a fixed Gaussian with a width a_n, which, is related to the De Broglie wavelength λ_n by $a_n = \lambda_n / 6$. The decoherence time in this approximation may be approximated by

$$\tau_d^{ht} = \left(\left\langle \delta\Omega_{12}^2 \right\rangle \int_0^\infty d\omega\, \tilde{J}_\Omega(\omega) \frac{(\beta\hbar\omega)^2}{12} \right)^{-1/2} . \tag{29}$$

Since the energy gap spectral density is known from the Fourier transform of $\tilde{C}_\Omega(t)$ (Fig. 2), the decoherence time can be computed for both water and methanol by numerical integration of the integrals in Eqs (28) and (29). The computed decoherence times are collected in Table II. For methanol, we find τ_d = 16.5 fs and τ_d^{ht} = 12.0 fs. This is very close to the results obtained recently by Turi and Rossky using the overlap between Gaussian wave packet trajectories starting from the excited state surface and propagating both on the excited and

ground state potential surfaces (τ_d = 16 fs and τ_d^{ht} = 13 fs, respectively).[51] A higher order expansion of the exponent with terms of order t^4 gives an effective decoherence time, τ_d = 14 fs. In agreement with previous findings[40,51] we computed shorter decoherence times for water than for methanol. For our simulation, the present formalism yields τ_d = 7.5 fs, τ_d^{ht} = 4.8 fs, in full agreement with the wave packet calculations of Prezhdo and Rossky.[40]

F. Quantized correlation functions and quantum transition rates: Frequency-dependent expression of the rate

We have seen that the non-adiabatic coupling is predominantly modulated by the solvent vibrations (Fig. 3). Since the average excited state energy gap for both methanol and water models falls just in the bending/stretching region of the solvent vibrational spectra, one could invoke resonance phenomena which would be responsible for the surprisingly high value of the non-adiabatic decay rates. In order to quantify this assertion and to estimate how much each region of the solvent vibrational spectrum contributes to the rates, it is convenient to express the rate in a frequency dependent rather than time dependent form. For this, we return to the initial quantum rate formula, Eq. (10). If cross-correlation terms are neglected, as suggested above, the transition rate can be expressed as

$$k_{1\to 2} = \frac{1}{\hbar^2} \int_{-\infty}^{\infty} dt\; e^{i\langle \Omega_{12} \rangle t} C_V^q(t) G^q(t)\,, \tag{30}$$

where $C_V^q(t)$ is the quantized coupling autocorrelation functions and $G^q(t)$ is the quantized dephasing exponential function. Now we can write $C_V^q(t)$ as a Fourier transform

$$C_V^q(t) = \frac{1}{2\pi} \int_{-\infty}^{+\infty} d\omega\, e^{i\omega t}\, \hat{C}_V^q(\omega)\,, \tag{31}$$

and substitute in Eq. (30). Performing the integration over *t* yields

$$k_{1\to 2} = \int_{-\infty}^{+\infty} d\omega\, \hat{k}(\omega)\,, \tag{32}$$

where $\hat{k}(\omega)$ gives the contribution of the frequency ω to the total rate. The frequency dependent rate contribution then reads as

$$\hat{k}(\omega) = \frac{1}{2\pi}\, \hat{C}_V^q(\omega)\, \hat{W}(\omega)\,, \tag{33}$$

where $\hat{W}(\omega)$ is a "window function" defined by

$$\hat{W}(\omega) = \int_{-\infty}^{+\infty} dt\; e^{i\langle\Omega_{12}\rangle t} G^q(t) \approx \sqrt{2\pi\left\langle \delta\Omega_{12}^2 \right\rangle_q}\; \exp\left\{ -\frac{\left(\omega - \langle\Omega_{12}\rangle\right)^2}{2\left\langle \delta\Omega_{12}^2 \right\rangle_q} \right\}. \tag{34}$$

The last equation follows from the previously discussed Gaussian approximation. Note, that following the time domain formulation of Eqs (12)-(23), another equivalent interpretation of the rate in Eqs (32)-(34) is the convolution, in frequency space, of the coupling correlation function $\hat{C}_V^q(\omega)$ by the dephasing function $\hat{G}^q(\omega)$, evaluated at the mean frequancy $\langle\Omega_{12}\rangle$. Using preferably the Gaussian window picture with the harmonic quantization scheme, the following final expression is reached for $\hat{k}(\omega)$:

$$\hat{k}(\omega) = \sqrt{2\pi\left\langle \delta\Omega_{12}^2 \right\rangle_q}\; \frac{\beta\hbar\omega}{1-e^{-\beta\hbar\omega}}\; J_V(\omega)\, \exp\left\{ -\frac{(\omega - \langle\Omega_{12}\rangle)^2}{2\left\langle \delta\Omega_{12}^2 \right\rangle_q} \right\} \tag{35}$$

A similar expression arises if the alternative standard quantization scheme of Eqs (21) is employed instead. In Fig. 6, we have displayed the frequency dependent rate, $\hat{k}(\omega)$, for water and methanol, together with the window function, $\hat{W}(\omega)$. It can be checked again that there is an important factor (~10) between the classical answer (obtained by suppressing the mode renormalization factor $\frac{\beta\hbar\omega}{1-e^{-\beta\hbar\omega}}$ in Eq. (35)) and the harmonic quantized answers. The standard quantization predicts a more moderate increase (a factor of 2) of the rates relative to

those quoted in the preceding section. We think that the harmonic quantization procedure is more appropriate here, since the contributing modes are vibrational. It is nonetheless reassuring that a different quantization procedure produces similar trends in decay rates.

In a more general context, we remark that the time dependent golden rule is often understood as a way to extract the bath-modulated coupling contribution *at the mean frequency* of the quantum subsystem. This is the essence of the Landau-Teller formula for vibrational energy relaxation.[72,73] In our case, this statement means looking at the resonant frequencies $\overline{\omega} = \langle \Omega_{12} \rangle \approx 3400\ \mathrm{cm}^{-1}$ for water, and $\overline{\omega} = \langle \Omega_{12} \rangle \approx 2300\ \mathrm{cm}^{-1}$ for the present model of methanol. In the latter case, very little spectral contribution is found since this frequency falls in between the bending and stretching peaks. However, we find that the window function is quite broad in both cases, and the whole vibrational spectrum contributes almost equally to the overall rate. For water, the O-H stretching mode appears more favored, whereas for methanol the window function enhances the bending mode and dampens somewhat the stretching mode contribution. Therefore, it appears crucial here to go beyond the Landau-Teller approximation. We believe that this statement may also be true for the vibrational relaxation of H-bonded systems, where substantial band broadening effects are to be taken into account.

G. Discussion

As pointed out previously, the different pseudopotentials and the different classical interaction potential models may lead to substantially different rates mainly through the mean value of the coupling, $\langle V_{12}^2 \rangle$, and the average electronic energy gap, $\langle \Omega_{12} \rangle$. The following discussion illustrates this complex dependency on the example of the excited state hydrated electron.

Most of the pseudopotentials are selected based on ground state properties. Thus, the electronic gap when the excited state is occupied may be in error. Since the average gap appears explicitly in the various rate formulas derived previously, one can easily evaluate the effect of varying this quantity, with the assumption that fluctuations remain the same. In the frequency dependent formulation of Eqs (32)-(35) illustrated by Fig. 6, this amounts to shifting the window function while keeping the Fourier decomposition of the coupling correlation function unchanged. Furthermore, the coupling strength appears strongly correlated with the energy gap. This fact is already apparent in Fig. 1 and is further illustrated in Fig. 7 where we have plotted the probability distribution of the excited state energy gap of the hydrated electron, $P(\Omega)$, and the average value of V_{12}^2 sampled at each particular energy value Ω, denoted by $V_{12}^2(\Omega)$. $V_{12}^2(\Omega)$ decreases sharply up to about 0.5 eV, and then tends to zero more gradually. Averaging this quantity over the energy gap distribution yields the average value quoted in Table I; that is

$$\left\langle V_{12}^2 \right\rangle = \int_0^\infty d\Omega \, V_{12}^2(\Omega) \, P(\Omega). \qquad (36)$$

We also note that $P(\Omega)$ can be well approximated by a Gaussian distribution (see Fig. 7). To examine the impact on rates of this correlation between coupling and energy gap, we simply retain Eq. (36) and consider a simple shift in the energy gap distribution with changes in $\left\langle \Omega_{12} \right\rangle$. This provides an appropriate scaled coupling strength which depends on the average energy gap, $\left\langle V_{12}^2 \right\rangle\left(\left\langle \Omega_{12} \right\rangle\right)$, and we can estimate the overall variation of the decay rate with the average energy gap from Eqs (32)-(35). Fig. 8 shows the lifetime of the excited state electron as the function of the average energy gap for the classical case, as well as for the standard and harmonic quantization schemes. For the last case we also included a curve where the contributions of the very high frequency coupling (above 5500 cm^{-1}), which are likely to be overemphasized by the harmonic quantization formula, have been removed. The excited state

lifetime is seen to increase sharply with increasing average energy gap. For the standard procedure, which can be considered as the minimal quantum correction scheme, the lifetime reaches 1 ps by about 0.8 eV, while the harmonic approximation still predicts sub-100 fs lifetimes in a similar energy range. While we believe that the harmonic approximation is justified in the present context, the finding of a 4 fs excited state lifetime, a time shorter than any other relaxation timescale of the system, is unphysical, and points to an inconsistency in this application of the equilibrium golden rule expression. The larger amplitude of the quantum solvent vibrational modes that follows vibrational quantization should increase the rate, but this effect seems overestimated in the harmonic approximation.

With the previous considerations in mind it is important at this point to return to our bare numerical results (Table II) and put them into perspective of time resolved spectroscopy. For water and methanol, our computed excited state electron lifetimes are extremely short, especially within the harmonic quantization procedure: a few femtoseconds for water, and around 20 fs for methanol. In a simple three-step picture of electronic relaxation after an ultrashort excitation pulse, the solvent begins by relaxing to adapt the electron cavity to the new electronic state. After complete relaxation, the p-s energy gap is minimal and a radiationless transition can occur with maximum probability. After the electronic transition, the solvent relaxes to the newly formed equilibrium ground state electronic distribution. With our computed rates, the second step appears quasi-instantaneous and the whole dynamics is driven by solvent relaxation. If linear response applies (which was verified in the present work for water, and by Mosyak *et al.* for methanol[49]), the excited state solvent relaxation occurs in water with a fast 10 fs inertial response followed by a ~300-700 fs exponential decay, and in methanol with a similarly fast initial Gaussian decay of 20 fs followed by a slower biexponential response with characteristic times of 1 and 7 ps (see Fig. 2). The ground state relaxation occurs with more or less the same characteristic times. If one assumes that the

above scenario is idealized, then non-adiabatic transitions can occur before the excited state equilibrium is reached yielding an effective transition time which appears longer. Nonetheless, we can anticipate from our results and the expected energy gap dependence of the decay time (Fig. 8) that the electronic population dynamics will be dictated by solvent dynamics. Regarding the possibility of very short population decay times, we do note that Pshenichnikov *et al.* invoke a 50 fs excited state lifetime to interpret their photon echo experiments with ultrafast 5-fs pulses,[61] and similar lifetimes have been predicted by Zharikov and Fischer using a continuum solvated electron model.[74] However, it is difficult to reconcile these with excited state electron scavenging experiments,[75] which appear to provide a more direct interrogation of an electronic state survival.

IV. Conclusion

We have introduced a new time dependent form of the Fermi golden rule involving quantum time correlation functions which can be evaluated by alternate routes, the easiest being to infer them from their classical counterparts, followed by a suitable quantization scheme. When applied to the problem of the lifetime of an equilibrated p-electron in water or methanol, this formulation has permitted us to reach some important conclusions: (i) For this problem, the neglect of the cross-correlation function between the value of the non-adiabatic coupling and energy gap is well justified by the ultrafast dephasing. With a Gaussian approximation of the dephasing function, we obtain a rather simple and transparent rate formula in either the time or frequency domain. (ii) The non-adiabatic transition appears to be entirely driven by the coupling of the electron to the vibrational modes of the solvent. (iii) Quantum effects are substantial and increase the rate by approximately one order of magnitude with respect to a fully classical treatment of the nuclear degrees of freedom. (iv) In

contrast to a Landau-Teller formula with a single solvent frequency governing the rate, the whole vibrational spectrum turns out to contribute almost equally to the electronic relaxation rate. (v) In contrast to previous theoretical studies which explicitly considered the non-equilibrium experimental process, the current equilibrium golden rule approach predicts extremely short equilibrated p-electron lifetimes. These contrasting results suggest that the electronic relaxation after an ultrashort photoexciting pulse is, in fact, heavily influenced by solvent reorganization dynamics.

We believe that the new Fermi golden rule formulation presented here can be useful for other problems involving quantum transitions in condensed phases, for example vibrational relaxation in H-bonded molecular systems. On the other hand, we have seen that the equilibrium golden rule may have reached its limits for the present problem, and non-perturbative approaches and non-equilibrium golden rule methods should be also considered in the future.[76,77]

Acknowledgments

This work was supported by research grants to LT from the Eötvös Fellowship, the Bolyai Research Fellowship, and from the National Research Fund of Hungary (OTKA, T049715). PJR acknowledges the support of the U. S. National Science Foundation (CHE-0134775), and the R. A. Welch Foundation (F-0019).

References

[1] V. May , and O. Kühn, Charge and Energy Transfer Dynamics in Molecular Systems (Wiley-VCH, Weinheim, 2004).

[2] R. Car and M. Parrinello, Phys. Rev. Lett. **55**, 2741 (1985).

[3] M. Sprik and M. L. Klein, J. Chem. Phys. **89**, 1592 (1988).

[4] J. C. Tully, J. Chem. Phys. **93**, 1061 (1990).

[5] E. Neria, A. Nitzan, R. N. Barnett, and U. Landman, Phys. Rev. Lett. **67**, 1011 (1991).

[6] A. Staib and D. Borgis, J. Chem. Phys. **103**, 2642 (1995).

[7] F. A. Webster, P. J. Rossky, and R. A. Friesner, Comput. Phys. Commun. **63**, 494 (1991).

[8] K. F. Wong and P. J. Rossky, J. Chem. Phys. **116**, 8418 (2002).

[9] K. F. Wong and P. J. Rossky, J. Chem. Phys. **116**, 8429 (2002).

[10] E. Neria and A. Nitzan, J. Chem. Phys. **99**, 1109 (1993).

[11] R. Kubo and Y. Toyozawa, Prog. Theor. Phys. **13**, 160 (1955).

[12] R. Kubo, Adv. Chem. Phys. **15**, 101 (1969).

[13] P. Schofield, Phys. Rev. Lett. **4**, 239 (1960).

[14] P. A. Egelstaff, Adv. Phys. **11**, 203 (1962).

[15] B. J. Berne and G. D. Harp, Adv. Chem. Phys. **17**, 63 (1970).

[16] D. W. Oxtoby, Adv. Chem. Phys. **47**, 487 (1981).

[17] P. H. Berens, S. R. White, and K. R. Wilson, J. Chem. Phys. **75**, 515 (1981).

[18] J. S. Bader and B. J. Berne, J. Chem. Phys. **100**, 8359 (1994).

[19] H. Kim and P. J. Rossky J. Phys. Chem. B **106**, 8240 (2002).

[20] S. A. Egorov, E. Rabani, and B. J. Berne, J. Chem. Phys. **110**, 5238 (1999).

[21] S. A. Egorov, E. Rabani, and B. J. Berne, J. Phys. Chem. **103**, 10978 (1999).

[22] S. A. Egorov, K. F. Everitt, and J. L. Skinner J. Phys. Chem. A **103**, 9494 (1999).

[23] A. Warshel and J.-K. Hwang, J. Chem. Phys. **84**, 4938 (1986).

[24] J. S. Bader, R. A. Kuharski, and D. J. Chandler, Chem. Phys. **93**, 230 (1990).

[25] J.-K. Hwang and A. Warshel, Chem. Phys. Lett. **271**, 223 (1997).

[26] C. D. Jonah, C. Romero, and A. Rahman, Chem. Phys. Lett. **123**, 209 (1986).

[27] A. Wallqvist, D. Thirumalai, and B. J. Berne, J. Chem. Phys. **86**, 6404 (1987).

[28] A. Wallquist, G. Martyna, and B. J. Berne, J. Phys. Chem. **92**, 1721 (1988).

[29] E. Gallicchio and B. J. Berne, J. Chem. Phys. **10**, 7064 (1996).

[30] R. N. Barnett, U. Landman, C. L. Cleveland, and J. Jortner, J. Chem. Phys. **88**, 4421 (1988).

[31] R. N. Barnett, U. Landman, C. L. Cleveland, and J. Jortner, J. Chem. Phys. **88**, 4429 (1988).

[32] J. Schnitker and P. J. Rossky, J. Chem. Phys. **86**, 3462 (1987).

[33] J. Schnitker, K. Motakabbir, P. J. Rossky, and R. Friesner, Phys. Rev. Lett. **60**, 456 (1988).

[34] B. J. Schwartz and P. J. Rossky, J. Chem. Phys. **101**, 6902 (1994).

[35] B. J. Schwartz and P. J. Rossky, J. Chem. Phys. **101**, 6917 (1994).

[36] B. J. Schwartz and P. J. Rossky, J. Chem. Phys. **105**, 6997 (1996).

[37] O. V. Prezhdo and P. J. Rossky, J. Phys. Chem. **100**, 17094 (1996).

[38] B. J. Schwartz, E. R. Bittner, O. V. Prezhdo, and P. J. Rossky, J. Chem. Phys. **104**, 5942 (1996).

[39] E. R. Bittner and P. J. Rossky, J. Chem. Phys. **107**, 8611 (1997).

[40] O. V. Prezhdo and P. J. Rossky, J. Chem. Phys. **107**, 5863 (1997).

[41] O. V. Prezhdo and P. J. Rossky, Phys. Rev. Lett. **81**, 5294 (1998).

[42] C.-Y. Yang, K. F. Wong, M. S. Skaf, and P. J. Rossky, J. Chem. Phys. **114**, 3598 (2001).

[43] S. Bratos and J.-C. Leicknam, Chem. Phys. Lett. **261**, 117 (1996).

[44] S. Bratos, J.-C. Leicknam, D. Borgis, and A. Staib, Phys. Rev. E **55**, 7217 (1997).

[45] L. Turi, M. P. Gaigeot, N. Lévy, and D. Borgis, J. Chem. Phys. **114**, 7805 (2001).

[46] L. Turi and D. Borgis, J. Chem. Phys. **114**, 6186 (2002).

[47] J. Zhu and R. I. Cukier, J. Chem. Phys. **98**, 5679 (1993).

[48] L. Turi, A. Mosyak, and P. J. Rossky, J. Chem. Phys. **107**, 1970 (1997).

[49] A. A. Mosyak, O. V. Prezhdo, and P. J. Rossky, J. Chem. Phys. **109**, 6390 (1998)

[50] P. Mináry, L. Turi, and P. J. Rossky, J. Chem. Phys. **110**, 10953 (1999).

[51] L. Turi and P. J. Rossky, J. Chem. Phys. 120, 3688 (2004).

[52] A. Migus, Y. Gauduel, J. L. Martin, and A. Antonetti, Phys. Rev. Lett. **58**, 1559 (1987).

[53] F. H. Long, H. Lu, and K. B. Eisenthal, Phys. Rev. Lett. **64**, 1469 (1990).

[54] Y. Gauduel, S. Pommeret, and A. Antonetti, J. Phys. Chem. **97**, 134 (1993).

[55] J. C. Alfano, P. K. Walhout, Y. Kimura, and P. F. Barbara, J. Chem. Phys. **98**, 5996 (1993)

[56] P. J. Reid, C. Silva, P. K. Walhout, and P. F. Barbara, J. Phys. Chem. **98**, 3450 (1994).

[57] K. Yokoyama, C. Silva, D. H. Son, P. K. Walhout, and P. F. Barbara, J. Phys. Chem. A **102**, 6957 (1998).

[58] C. Silva, P. K. Walhout, K. Yokoyama, and P. F. Barbara, Phys. Rev. Lett. **80**, 1086 (1998).

[59] M. Assel, R. Laenen, and A. Laubereau, J. Phys. Chem. A **102**, 2256 (1998).

[60] M. Assel, R. Laenen, and A. Laubereau, Chem. Phys. Lett. **317**, 13 (2000).

[61] M. S. Pshenichnikov, A. Baltuska, and D. W. Wiersma, Chem. Phys. Lett. **389**, 171 (2004).

[62] X. Shi, F. H. Long, H. Lu, and K. B. Eisenthal, J. Phys. Chem. **99**, 6917 (1995).

[63] P. K. Walhout, J. C. Alfano, Y. Kimura, C. Silva, P. Reid, and P. F. Barbara, Chem. Phys. Lett. **232**, 135 (1995).

[64] D. M. Lockwood, H. Hwang, and P. J. Rossky, Chem. Phys. **268**, 285 (2001).

[65] D. M. Lockwood, Y.-K. Cheng, and P. J. Rossky, Chem. Phys. Lett. **345**, 159 (2001).

[66] A. Nitzan and R. J. Silbey, J. Chem. Phys. **60**, 4070 (1974).

[67] D. Borgis, S. Lee and J.T. Hynes, Chem. Phys. Lett. **162**, 19 (1989).

[68] D. Borgis, G. Tarjus, and H. Azzouz, J. Phys. Chem. **96**, 3188 (1992).

[69] D. Borgis, in Ultrafast Reaction Dynamics and Solvent Effects, Y. Gauduel and P. Rossky eds (AIP Press, New York, 1994), p205.

[70] S. Mukamel, Nonlinear Optical Spectroscopy (Oxford University Press, New York, 1995).

[71] D. Borgis, unpublished.

[72] R. M. Whitnell, K. R. Wilson, and J. T. Hynes, J. Chem. Phys. **96**, 5354 (1992).

[73] K. F. Everitt, J. L. Skinner, and B. M. Ladanyi, J. Chem. Phys. **116**, 179 (2002).

[74] A. A. Zharikov and S. F. Fischer, J. Chem. Phys. **124**, Art. No. 054506 (2006).

[75] T. W. Kee, D. H. Son, P. Kambhampati, and P. F. Barbara, J. Phys. Chem. A **105**, 8434 (2001).

[76] R. D. Coalson, D. G. Evans, and A. Nitzan, J. Chem. Phys. **101**, 436 (1994).

[77] A. A. Golosov, and D. R. Reichman, J. Chem. Phys. **115**, 9848 (2001).

Tables

Table I. Averaged classical quantities collected along the MD runs, and the corresponding quantized quantities (denoted by the *q* subscript) computed using the harmonic quantization scheme. All quantities are in fs^{-1}.

	$\langle \Omega_{12} \rangle$	$\langle \delta\Omega_{12}^2 \rangle^{1/2}$	$\langle \delta\Omega_{12}^2 \rangle_q^{1/2}$	$\frac{1}{\hbar}\langle V_{12}^2 \rangle^{1/2}$	$\frac{1}{\hbar}\langle V_{12}^2 \rangle_q^{1/2}$
Water	0.65	0.24	0.28	0.067	0.187
Methanol	0.42	0.17	0.18	0.044	0.104

Table II. Classical and quantized non-adiabatic transition times, and dephasing times for electronic relaxation of an equilibrated excited state solvated electron in water and methanol (see text). The quantized rates are computed using either the harmonic (H), and the standard (S) quantization schemes. The classical dephasing times and the quantum decoherence times using the harmonic quantization are also shown. All quantities are in fs.

	Classical dephasing time	Non-adiabatic transition times			Quantum decoherence time (Eqs (28) and (29))	
	τ_{ϕ}	$\tau_{1\to 2}^{cl}$	$\tau_{1\to 2}^{q,H}$	$\tau_{1\to 2}^{q,S}$	τ_{d}	τ_{d}^{ht}
Water	4.1	60	4.0	30	7.5	4.8
Methanol	5.9	160	17	80	16.5	12

Figure captions

Figure 1. 10 ps slices of the trajectories obtained for water (top), and for methanol (bottom). In each frame, the top curve reports the time-dependent energy gap and, for clarity, the bottom one gives the absolute value of the coupling, with a minus sign to avoid overlaps.

Figure 2. Normalized energy gap correlation function for an equilibrated solvated p-electron in water (top), and in methanol (bottom).

Figure 3. Spectral density (in arbitrary units) of the non-adiabatic coupling in water (top), and in methanol (bottom).

Figure 4. Classical reactive flux correlation function for water (top), and methanol (bottom). The circles indicate the direct numerical integration of Eqs (12) and (17), whereas the solid line involves the Gaussian approximation for the dephasing function, $G(t)$, with neglect of the cross-correlation terms, as in Eq. (24).

Figure 5. Quantum reactive flux for water (top), and methanol (bottom). The solid line is for the direct integration of Eq. (22), including all terms, and the dashed line involves a Gaussian approximation for the dephasing function $G^q(t)$ and the neglect of the cross-correlation terms, Eq. (25). The dot-dashed line recalls the classical results of figure 4.

Figure 6. Frequency-dependent rate for water (top), and methanol (bottom). The solid curve indicates the quantized result using the harmonic quantization scheme, and the dashed-dotted

curves denote the standard quantization procedure (Eqs (20)-(23)). The Gaussian-like dashed curve on top is the "window" function of Eq. (34) (renormalized to fit in the figure).

Figure 7. The probability distribution of the energy gap, $P(\Omega)$, and its approximation by a Gaussian distribution (dashed, upper frame). The average value of V_{12}^2 sampled at each particular energy value Ω (lower frame).

Figure 8. The lifetime of the excited state electron for alternative approximations as a function of the mean energy gap (see text). Classical case (solid), standard (dashed), and harmonic quantization schemes (dotted). The harmonic quantization with the very high frequency coupling contributions removed is also shown (dash-dot).

Figure 1. Borgis, Rossky and Turi

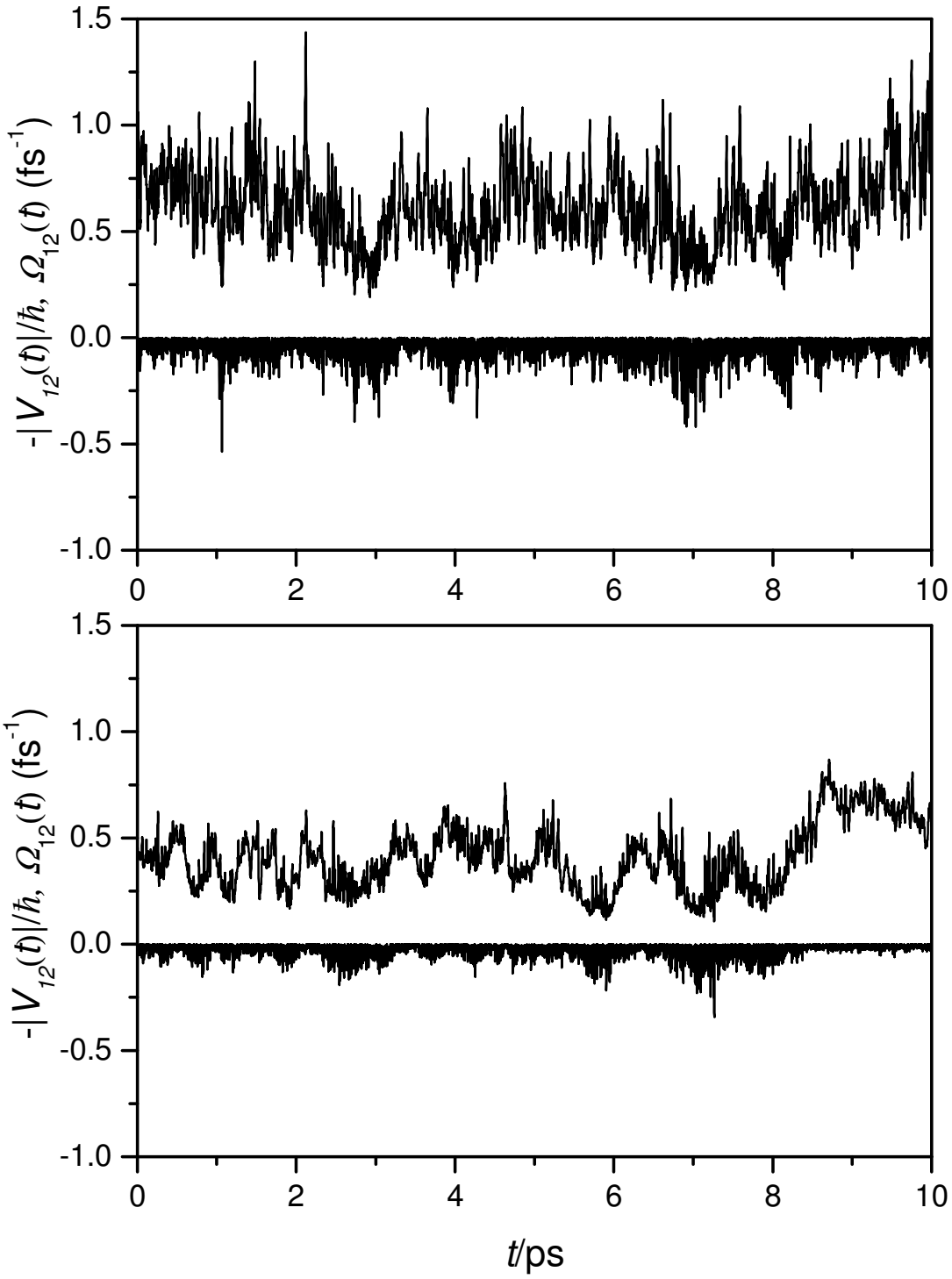

Figure 2. Borgis, Rossky and Turi

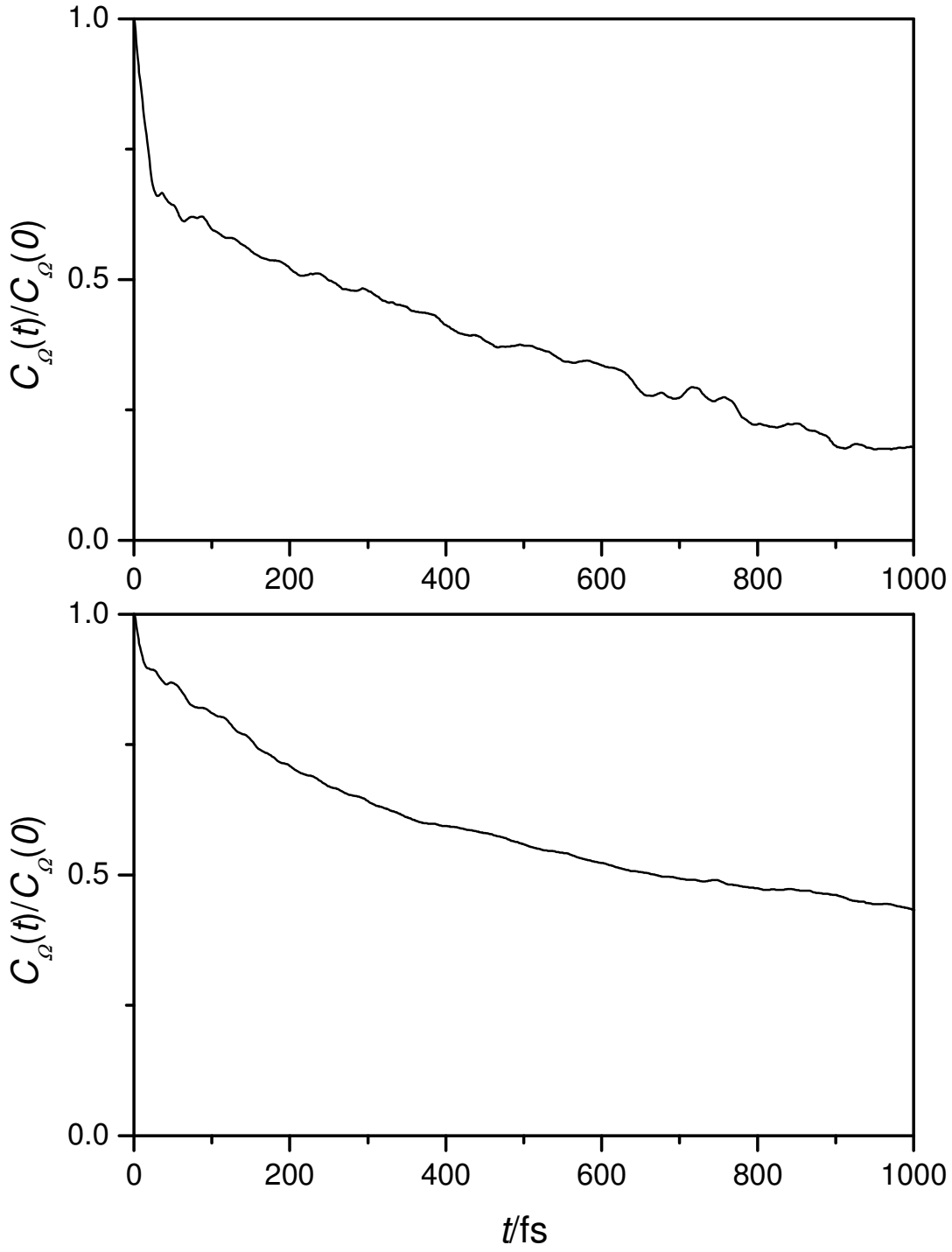

Figure 3. Borgis, Rossky and Turi

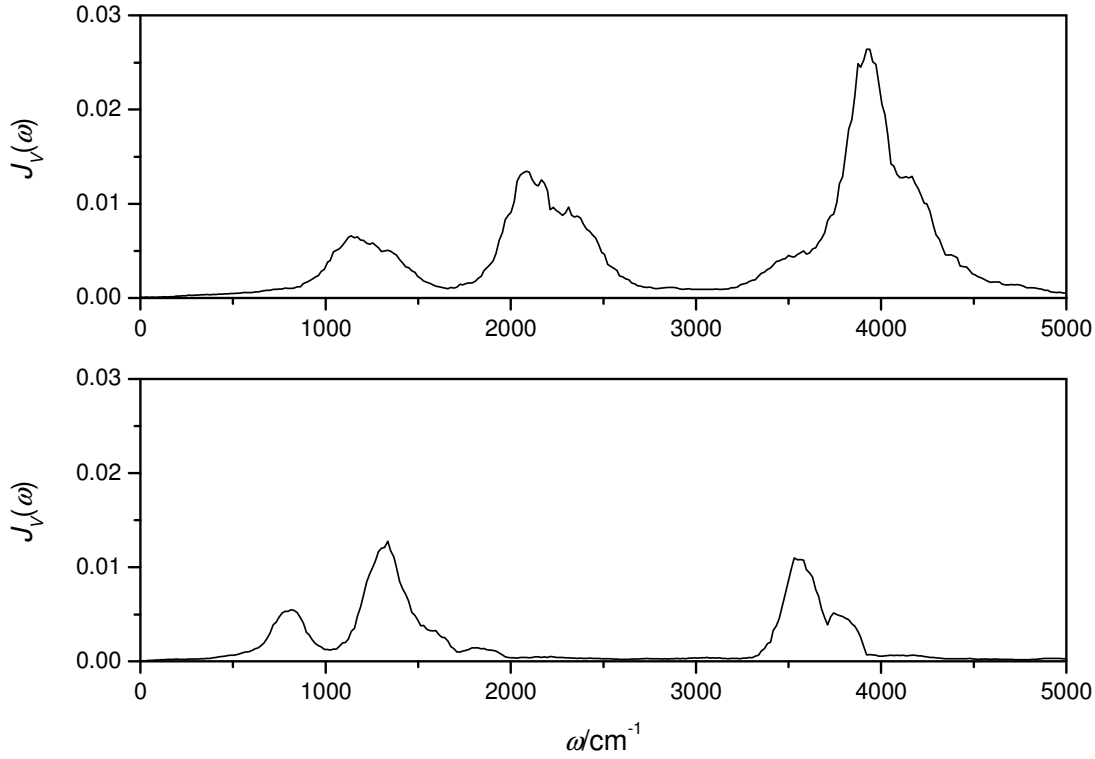

Figure 4. Borgis, Rossky and Turi

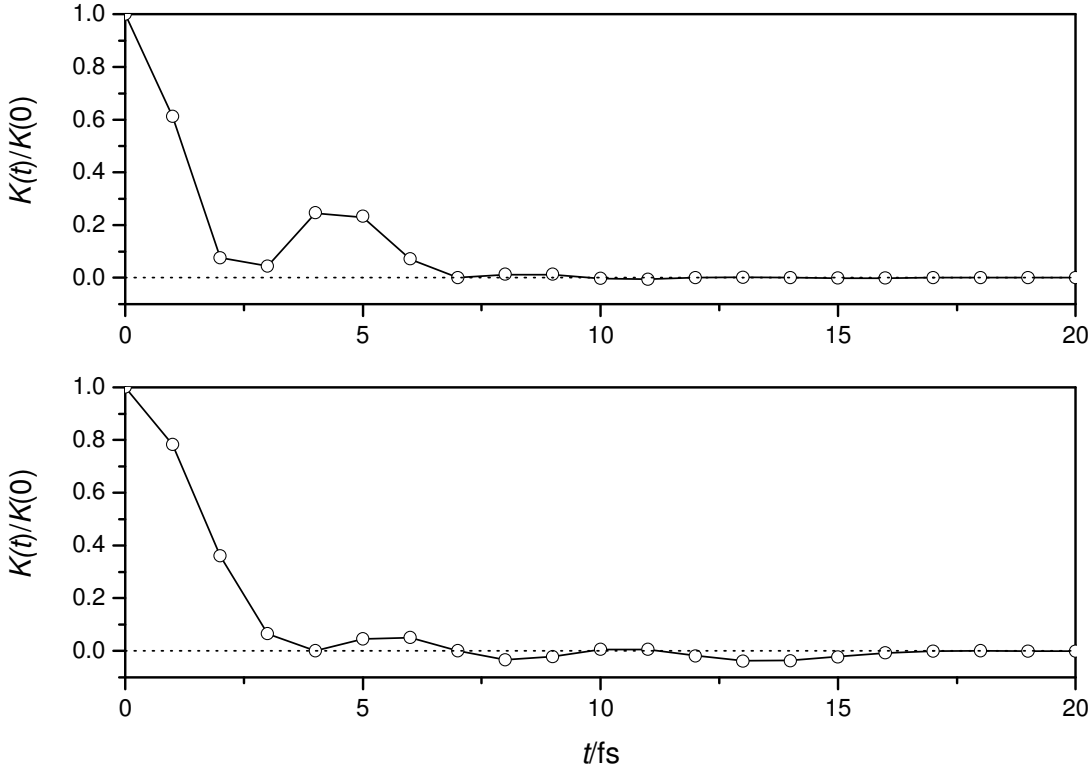

Figure 5. Borgis, Rossky and Turi

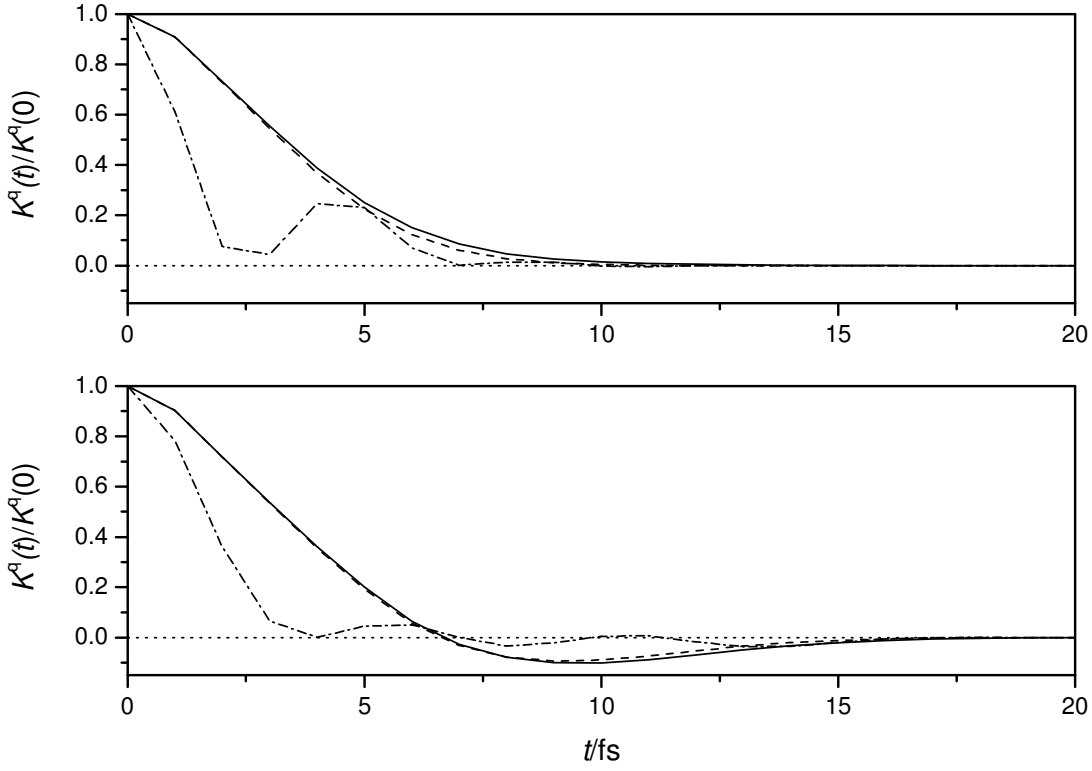

Figure 6. Borgis, Rossky and Turi

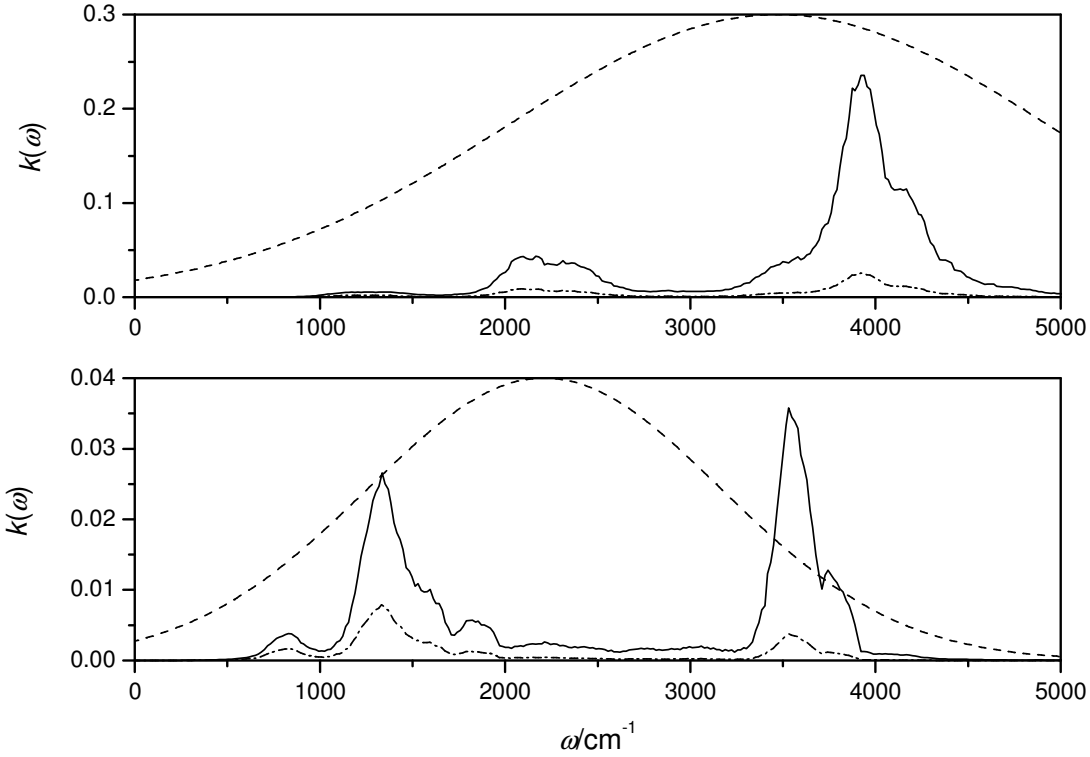

Figure 7. Borgis, Rossky and Turi

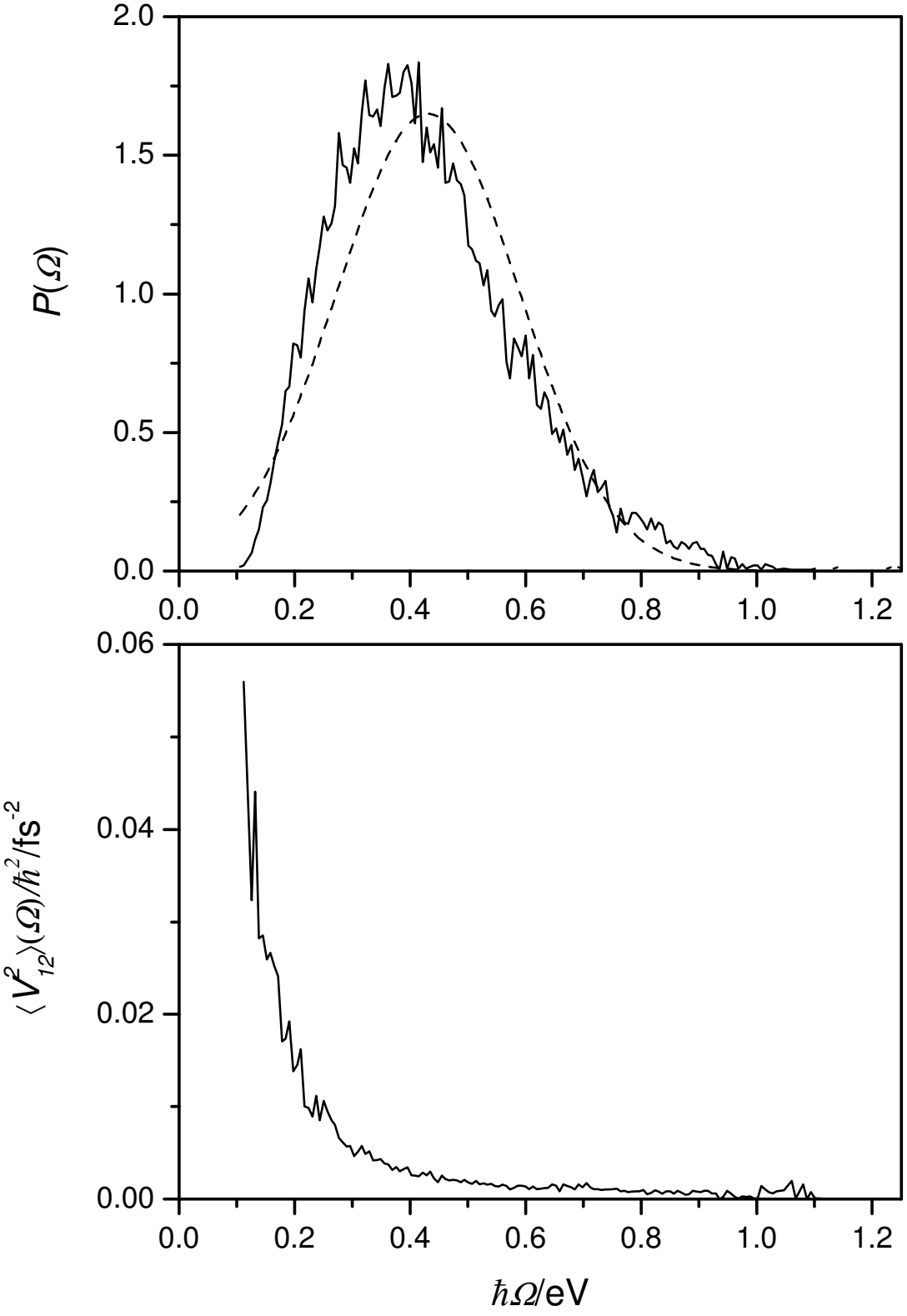

Figure 8. Borgis, Rossky and Turi